Polymer 49 (2008) 4150–4158

Contents lists available at ScienceDirect

Polymer

journal homepage: www.elsevier.com/locate/polymer

Evaluation of the phase composition of amylose by FTIR and isothermal immersion heats

P. Bernazzani*, V.K. Peyyavula, S. Agarwal, R.K. Tatikonda

Department of Chemistry and Physics, Lamar University, Beaumont, TX 77706, USA

ARTICLE INFO

Article history:
Received 20 February 2008
Received in revised form 7 July 2008
Accepted 7 July 2008
Available online 22 July 2008

Keywords:
Amylose
Phase composition
Immersion heats

ABSTRACT

Amylose, a linear component of starch, has been shown to be directly responsible for many of starch's physical properties. In this study isothermal DSC assisted by FTIR spectroscopy was used to determine the phase composition of amylose under various pH conditions and while shear was used to disrupt chain–chain interactions. The analysis was based on a three-phase model consisting of crystalline (type B and single helices), amorphous, and network (physical entanglements and hydrogen bonds related) environments. Varying the pH of the water present in the samples enables the detection of the presence of the networks. Such networks, preferentially located in the amorphous phase, were found to be more reactive to chemical and probably thermal modifications. However, when chain entanglements or hydrogen bond networks are found near or in the helix of the crystalline phase, the polymer becomes more resistant to chemical and physical modification. Furthermore, it was observed that pH and shear could be used to control the morphology, orientation and phase content of amylose, which had a significant impact on the biodegradability of the treated samples.

Published by Elsevier Ltd.

1. Introduction

The complete morphology of amylose, as well as its relation to the physical properties of the biopolymer is not well understood in the present state of knowledge [1]. Because of the large potential for commercialization [2,3], many studies have centered on this subject. The understanding of the molecular structure of amylose is a key to a better control of physical properties in order to custom-make samples for various applications such as building materials. Although the literature is increasingly complete on the different phases of each polysaccharide, the relationship at a molecular level, between the physical properties and amylose or amylopectin is still the subject of ongoing debates. The physical properties of starch are a mixture of distinct physical properties associated with amylose and amylopectin. One of the main properties of starch is called gelification, when the granules are heated in water at a temperature at which they undergo an irreversible swelling [4–7]; these swollen granules are embedded into a continuous matrix of entangled amylose. When these gels are stored they undergo a structural transformation called retrogradation in which the crystalline phase increases [8–10].

It is well established that amylose can crystallize in three usual forms denominated types A, B and V. Types A and B consist of double helix packing in an orthorhombic form with the A form being slightly deformed and dependent on the amount of water [15–24]. Type A is found mainly in tuber and while type B is mostly found in potato starch. Finally, type V is a single helix crystal form, which occurs only when amylose forms a complex with a suitable ligand such as *n*-butanol, iodine or fatty acids [15,18,25,26].

Most past studies use simplified models containing mostly of crystalline and amorphous regions. Some recent studies [17,26] have added to this model by differentiating between long-range and short-range ordered crystals, meaning some regions can behave in a crystalline fashion, but only over very limited region of space.

Some studies have shown that chain entanglements in polyolefins were responsible for many phenomena associated with gels and birefringence and were readily observable [27–29]. The presence of a large fraction of entangled polymer may also explain the seemingly erratic behavior of biopolymers. In amylose, the well documented phenomenon of birefringence, gelation and retrogradation cannot be explained using a two phase system consisting of distinct purely crystalline and amorphous components, but can follow a model showing an intermediate phase linking the two others. This third phase, found preferentially in the amorphous regions but also as defects in the crystalline phase, is believed to be the result of entanglements.

In this study, we will consider the network and evaluate their importance on the properties of amylose. We start by supposing that the network phase can be subdivided into two parts. While

* Corresponding author. Tel.: +1 409 880 8272; fax: +1 409 880 8270.
E-mail address: paul.bernazzani@lamar.edu (P. Bernazzani).

0032-3861/$ – see front matter Published by Elsevier Ltd.
doi:10.1016/j.polymer.2008.07.022

a physical network consists of entanglements between the chains, the presence of a hydrogen bonds network could be the results of the important number of OH groups in polysaccharides. This latter network serves as the main stabilizing agent of the crystalline forms. These hydrogen bonds have been reported to exist in intramolecular form or as intermolecular bridges between the chains [30–33], hence we emit the hypothesis that these latter also stabilize the entanglements between the chains.

In this paper, we have focused our attention on amylose for the two following reasons: (a) the linearity of the polymer simplifies the interpretation of data; (b) the fact that amylose is semi-crystalline and linear makes it largely responsible for the many of starches' properties [11–14] (gelation, enzyme resistance, retrogradation, etc.).

Our approach to the molecular structure determination and control of amylose is based on the importance of the non-crystalline phases, i.e. both the free chains and the entangled non-crystalline amylose. These mobile parts of the polymer have been shown to influence the rate of crystallization (affected by high temperature treatments), the gelation process as well as the initial increase in firmness at the start of the retrogradation process [15,24,34,35]. Mobility is crucial to these properties.

To understand the morphology of the network phases and their influence on the physical properties of the material, we need a method capable of easily varying the phase composition while minimizing alterations to the structure of the sample. Three major techniques have been used. (1) Thermal treatments have been shown to significantly modify the physical properties as well as the morphology and the structure of biopolymer chains [10,18,19,22,31]. This method may involve complex changes caused by the non-equilibrium state of the non-crystalline regions. (2) Using samples of various polymerization degrees is another method that has been used [35–37]. This technique seems to yield good results; however, difficulties inherent to polymers, such as polydispersity and the morphological differences caused by the methodologies of separation of the different chain lengths, increase the complexity of the interpretation. (3) Measuring heats of immersion. This third method consists of immersing the sample in solutions with varying pHs. While at extreme pHs, problems similar to those previously mentioned (polydispersity, etc.) might be encountered, these changes are gradually monitored thereby facilitating the interpretation. Another useful advantage of using pH modifications consists in the effect it will have on the hydrogen bond network as well as on the stability of other phases because the crystalline helical structures are stabilized by intra- and intermolecular hydrogen bonds.

In this paper, we investigate the morphology and phase content modification of amylose as a function of pH and shear stress, paying particular attention to the often-neglected presence of chain entanglements. Two methods will be correlated: FTIR spectroscopy and isothermal immersion heat measurements. The latter technique will help to determine the presence and origin of networks. Because entanglements restrain the freedom of the chains, a short-range order phase has been observed by ^{13}C NMR [23,24] and by FTIR [17,25,26,33] and associated with a mobility intermediary to the crystalline and to the perfectly amorphous phases. Taken to the extreme, these entanglements can produce crystallization between the knots in the event that this physical network is under stress, as is likely when the polymer is swollen in a solvent or by slowly increasing the temperature. The mobility of the various components will be investigated using polarized IR in a strained polymer environment.

DSC can observe the slow kinetics of disordering only if the heating ramp is very slow (a few degrees per hour), which leads to variations in the network fraction that are dependent of the heating rate. The technique of isothermal DSC to measure the immersion heats in water at various pHs was employed because these kinetic variations of the different phases would then be less significant on the results. As will be discussed, this method gives a surprisingly accurate way of estimating the modifications on physical properties that any treatment would have on the sample. It is therefore a good standard against which to gage the more complex information given by IR measurements. Quantitative evaluations of the morphological modifications were established with this method.

FTIR is known to distinguish vibrations in different environment. The region of CO bending vibrations (1300–800 cm^{-1}) has shown a relation with the water content and the crystalline (types B and V) and amorphous phases [17,25,26,34].

As we wish to investigate the effects of hydrogen bond networks, it might seem reasonable to observe the O–H stretching region (3200 cm^{-1}). However, our goal is to compare the various morphologies present in the polymer. The C–O bending region has been found to be sensitive to both the crystalline and amorphous environments. We have observed that this region is also sensitive to the physical network environment under certain conditions [15,34].

2. Experimental

2.1. Materials

Amylose isolated from potato starch was obtained from Sigma (St. Louis). No further purification steps were done, leaving some fatty acids residue, which may cause the formation of V type crystals. The samples were thoroughly dried under vacuum and P_2O_5 at room temperature for at least 12 h to enable precise control of water content. The X-ray spectra of these dry samples reveal their almost fully amorphous nature.

2.2. Calorimetry

All isothermal studies were performed on a C80 differential scanning calorimeter (DSC) from Setaram. A known weight of the completely dried sample was sealed under vacuum in an easily breakable glass tube. The heat generated by the breaking was, on average, 225 mJ. The tube was then immersed in 2 mL of an aqueous solution maintained at the desired pH. The reference contained an equal amount of both the glass and the solution. As all isothermal measurements were performed at 30 °C, an equilibrium time was required after which the actual breaking was done. An average of 40 min was needed to obtain thermal equilibrium after the immersion at which point the experiment ended.

2.3. Fourier transform infrared spectroscopy

A Thermo-Nicolet Nexus 470 spectrometer was used in transmission mode at a resolution of 1 cm^{-1} with 100 scans. In order to eliminate the large water interference in the spectra as well as for the reasons stated above, the CO bending vibrations (1300–800 cm^{-1}) were investigated. The sampling technique was as follows: a water solution at a desired pH was added to the dried amylose until 30% water weight by weight was achieved. The sample was then thoroughly mixed forming a paste, a quantity of which was placed between AgCl windows and the spectra taken. Strained samples were obtained by depositing the amylose on aluminum plates before a crude shear was applied between the plates. The samples were then placed on the AgCl windows for the IR measurements.

2.4. Spectral simulations

Because the peaks in the region of interest strongly overlap, spectral simulations were used to resolve the bands. The various

peak areas were then quantitatively determined. The simulations were carried out similarly on every sample. Prior to simulation, a linear baseline was established in the region of interest. The self-deconvolution and second derivative analysis were then performed. From these, the position and number of peaks were estimated. No further pre-treatments were performed on the spectra. All simulations were performed using eight bands. Based on the well-resolved band at 1078 cm^{-1}, each peak was attributed a full width at half height between 20 and 30 cm^{-1}.

3. Result and discussion

The objective of this study is to evaluate the effect of changes in phase morphology and more specifically the importance of the physical network on the physical properties of amylose. The first step is to quantitatively determine the relative amount of the various phases in samples of amylose. Two well-known methods will be used to perform this evaluation: isothermal heats of immersion measurements and infrared spectroscopy.

3.1. Isothermal heats of immersion

A relatively simple way to trace phase content and differences in morphology is to measure the heats of immersion of treated amylose samples using isothermal calorimetry. The simplest chemical treatment involves variations in the water's pH. As was described in Section 2, this method consists in preparing a sealed under-vacuum glass tube containing the sample and breaking it in the solution, the sample is then instantly immersed, with an associated measurable heat.

Fig. 1 shows a typical DSC trace of the immersion of amylose in water (pH = 7). Once the system is stabilized, the break is performed (at about 500 s) giving rise to a very sharp and small endothermic heat before quickly rising in an exothermic peak that lasts for about 2000 s (≈35 min). The initial endotherm can be explained in the following way: at the moment of breaking, the water penetrates the glass tube driven by the vacuum inside. The difference in vapor pressure gives rise to a sudden evaporation of the solution, which is observed as a small endotherm. This heat is quickly compensated by the exothermic heat associated with the breaking of the glass. This heat of breaking was found to vary between 190 and 250 mJ with an average value of 225 mJ. This amount was subtracted from the total heat generated by the immersion of the sample. The shape of the trace in Fig. 1 is the one most often encountered, however, because of the difficulty in obtaining perfectly identical glass tubes and therefore similar breaks, we also find band shapes where the contributions from the breaking of the glass and from the evaporation are not visible. This was not found to be a factor in the evaluation of the immersion heats as the immersion proper was virtually identical from sample to sample. The time to obtain complete immersion varied from instantly to 5 s.

Similar experiments were performed at a variety of pH. In order to obtain a quantitative determination of the changes in phase content the immersion heats were compared to those of two model molecules. The first, a-D-glucose, the monomer of amylose, was used in order to determine the effect of pH on the immersion heat of a sample with multiple OH groups. A second model molecule, maltose, originating from the enzymatic hydrolysis of starch, was used to verify the effect of the presence of an ether link on the immersion heat. By comparing the heats of immersion of these molecules with those of amylose, the phase content of the latter could be evaluated.

Fig. 2 shows the correlation between the immersion heats and pH for amylose, maltose and α-D-glucose. One notes that all values are exothermic, however, experimentally for α-D-glucose and maltose, an endothermic value is observed. This can be explained by the fact that, as both these molecules are soluble in water at the experimental temperature (30 °C), an endothermic heat of dissolution is added to the interaction heat that we wish to measure. In order to subtract this heat of dissolution, we estimated it by measuring the dissolution trace of both α-D-glucose and maltose in water at pH 7. Integration of the obtained trace gives the value to be subtracted from the immersion heat in order to obtain the exothermic heat of interaction of the sample.

Fig. 2 shows that the variation in α-D-glucose is relatively stable at lower pH with a value oscillating around −100 J/g. However, immersion in a basic solution diminishes the heat of interaction by 20%, from −100 to −78 J/g. This value is found over all basic pH tested, from 8.5 to higher. The decrease observed at higher pH is attributed to the solubilisation of the OH groups in the molecule and the disruption of the hydrogen bonds between the sample and water.

The trace of immersion heats of maltose as a function of pH gives a constant value of −100 J/g between the pH of 4 and 8. At pH lower than 4, we find an abrupt increase in the exothermic value, up to −121 J/g, indicative of the chemical hydrolysis of the sample into two molecules of glucose. At pH higher than 9, we find, as in α-D-glucose, that the heat of immersion is decreased to about −85 J/g. This is also associated to the chemical interactions between the alcohol group on the molecule and the $^{-}$OH found in the solution. Both traces of α-D-glucose and maltose in Fig. 2 give

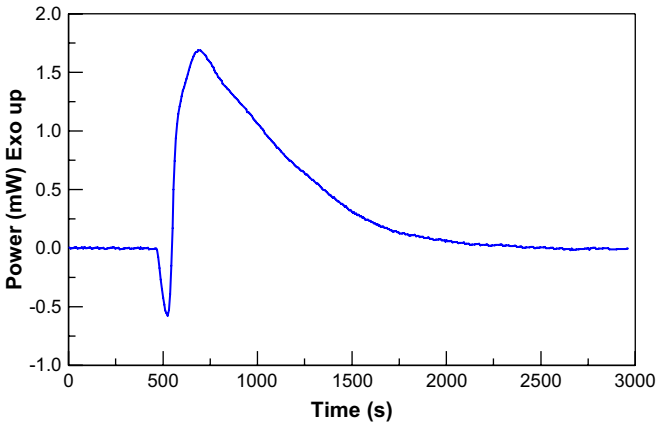

Fig. 1. DSC trace of amylose immersion in water (pH = 7).

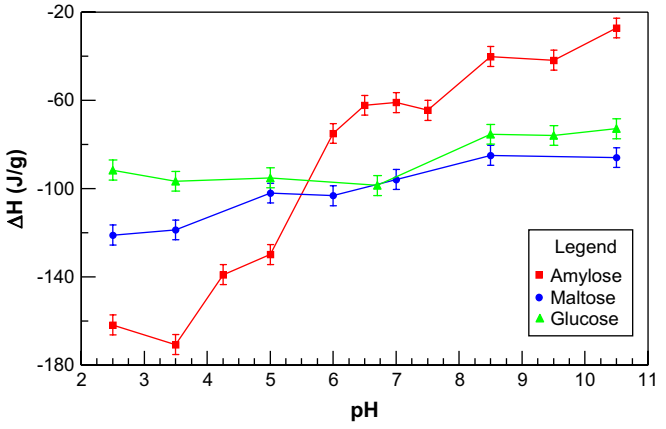

Fig. 2. Evolution of the immersion heat (Δ*H*) with increasing pH for three types of samples. The error bars represent the standard deviation from at least five measurements.

confidence in the resolving power of the technique of isothermal heats of immersion to identify changes in the structure of samples.

Fig. 2 also shows the variations with pH of the heat of immersion of amylose. Relatively large variations are observed with increasing pH. Near neutral pH values, the heat of immersion is intermediate. Increasing the pH to 8.5 decreases this heat to about −40 J/g, and remains at this value for all higher pH. Lowering the pH corresponds to a gradual increase of the exothermic peak up to a maximum of −176 J/g at a pH of 3.5. By comparing the traces of amylose and of maltose, we can emit the hypothesis that the hydrolysis of the acetylic bonds probably starts at a higher pH (between pH 4 and 5) but is not a gradual change. At a basic pH, we also attribute the decrease in exothermic heat to the solubilisation of the OH group in the molecule and the disruption of the hydrogen bonds between the sample and water, as was found in both α-D-glucose and maltose.

The large variations in amylose observed in Fig. 2, relative to maltose and glucose can lead to an estimation of the physical composition of the sample. Lets recall that, as previously stated, amylose is composed of an amorphous phase, i.e. chains free from interactions with their environment, a network phase where chains are connected to each other by either physical entanglements or hydrogen bonds and possibly two crystalline phases, one where the single chains form a single helix, the other, type B crystals, where chains assemble in double helices. With the exception of the amorphous phase, hydrogen bonds play an important stabilization role in all these forms.

Based on this composition, we emit the hypothesis that at a pH between 2.5 and 6 the maxima observed can be attributed to the dissociation of the physical network. The entanglements between the polymer chains are the source of tension between the involved chains. The fact that the polymer swells upon immersion could explain the origin of this tension because pulling on the knots will create tension between the chains. This tension represents a point of weakness along the chain. Driven by the large difference in chemical potential, the acidic solution will preferentially attack this point in order to decrease the tension. This attack takes the form of the hydrolyzation of the acetylic bonds to divide the chains into numerous shorter pieces. Once the tension is significantly decreased, the entanglements are eliminated. The observed increase in the associated exothermic heat may be the result of the presence of larger amounts of interactions with water molecules.

At a pH higher than 8, the decrease in the exothermic peak can be explained by the disruption of the hydrogen bonds. The fact that this solubilisation heat is much more pronounced for amylose than for either of the model molecules is indicative of the change in morphology occurring as a consequence of the disappearance of the hydrogen bonds. Another possibility explaining this large increase in heat involves once more the presence of networks. These networks have been classified in two types, physical (entanglements) and chemical (hydrogen bonded). These later will be affected most in a higher pH solution. Here again the slight tension created by the presence of this chemical network destabilizes the region and renders it the most chemically reactive. These hydrogen bonds should therefore be the first removed at higher pH, which enables the evaluation of their relative amounts.

Based on these assumptions, we can quantitatively evaluate the relative phase content of the amylose sample by the change in immersion heat at various pH compared to those of the model molecules. Table 1 shows the estimated values. The untreated sample showed a 21% crystalline content and a 14% network content. Thermally treating the sample, i.e. heating it at 60 °C for 30 min and slowly allowing it to cool until room temperature, produced an increase in the crystalline content, while the network phase did not seem significantly affected. Placing a shear on the sample did increase the crystalline content but most importantly increased the network phase. This could be explained by the shear forcing the entangled chains in the direction of the shear and increasing the amount of strain in these regions.

Table 1
Phase composition distribution for different amylose samples determined by isothermal immersion heats

Amylose sample	Heat contribution from (%)		
	Crystalline	Amorphous	Network
Untreated	21	65	14
Thermally treated	30	58	12
Oriented	27	50	23

In order to confirm this evaluation, and the relative importance of the networks in amylose, FTIR spectroscopy was used to identify each of the components of amylose separately.

3.2. IR analysis

3.2.1. Band identification

A typical spectrum of amylose in the region of 1300–850 cm^{-1} is shown in Fig. 3 along with the spectral simulation necessary in order to resolve the bands that strongly overlap. This region is traditionally attributed to different types of transitions: the C–C stretching vibrations from 1200 to 1103 cm^{-1}, and to the C–O bending vibrations from 1047 to 994 cm^{-1} are two of the most prominent [12]. More specifically, some of the peaks have been tentatively attributed in the literature [12,25,26,34]. Three bands in the CO bending region were attributed; one to the amorphous phase environment, 1022 cm^{-1}, the single helix crystalline structure environment, 1002 cm^{-1}, and the type B crystal structure environment, 1047 cm^{-1}. In a previous paper [34], it was suggested that the bands at 1150 and 1123 cm^{-1} were attributed to network environments related, respectively, to entanglements and hydrogen bonds.

The simulated peaks' positions were followed as a function of pH and were compared to the variations in immersion heats. Fig. 4 shows the variation of the peak position for four bands, the type B crystals (A), the complexed crystals (B), the amorphous-related band (C), and the physical network (D). The variations in position are indicative of the modification in the strength of the bond involved in the vibration. As this strength increases, so does the band position. Several factors contribute to this effect. The most important factor is electron delocalization. This is varied when interactions with environing atoms favor or disrupt the electron flow, which makes some vibrational transitions sensitive to

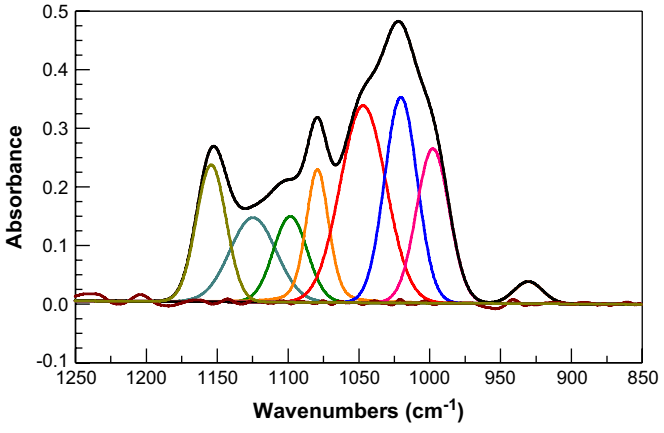

Fig. 3. FTIR spectrum of amylose in the 1300–850 cm^{-1} region. The spectral simulation and residual noise are also shown.

crystalline and/or amorphous environments. The bond strength can be modified if the vibrating group is in contact with hydrogen bonds from either inter- or intramolecular sources. A position variation should arise from the different location of the hydrogen bond, but it might be too small to resolve. A change in bond angles is the second major source of peak position variations as the electron delocalization will either be improved or impeded depending on the bond position. This is the foundation of the vibrational argument attributing the 1150 cm^{-1} band to the physical network as the strain caused by entanglements deforms the angle of the C–O vibration causing an increase in the position of this band.

The variations observed in the peak position of the C–O bending vibration in the type B crystals environment, Fig. 4A, shows a steady increase in bond strength at pH higher than 8 while the trace shows first a position increase at pH lower than 5, followed by a sharp decrease at values lower than 3. If this band is representative of the double helical type B crystals, the high pH variation can be explained by once again considering that the hydrogen bonds responsible for the stabilization of the double helix are slowly eliminated at higher pH since the inside of the helix is protected by the presence of the $^{-}$OH. The elimination of these hydrogen bonds is therefore a cooperative effort as the double helices slowly open up to let the $^{-}$OH groups inside be neutralized. The increase in "bond strength" is the result of this ionization of the COH bond as the bending of the C–O becomes more difficult. At lower pH the increase followed by the sudden decrease of the peak position can be related to the fact that the helical structure of the crystals also protects the hydrolyzation of the acetylic bonds; as the COC bonds located elsewhere in the sample are hydrolyzed, a deformation in the helical structure occurs, which increases the bending toughness of the C–O bonds. However, with lowering of the pH the hydrolyzation takes place and an abrupt decrease in peak position is observed. These variations seem to be in accordance with the assignment of this band to the type B crystal environment.

Fig. 4B follows the variation of peak position with the pH for the band assigned also to C–O bending vibrations but in a single helix crystal environment. Fig. 4B shows that the variation closely resembles that observed for the band in the type B crystal environment hinting to the fact that both bands are involved in similar conditions, possibly related to the helical structure that both favor. This might account for the assignment disparities found in the literature. At high pH (>7) a displacement of the peak position towards higher wavenumbers is observed. As in the type B crystal band, this can be explained by the fact that the efficiency of the hydrogen bonds, responsible for the stability of the complexed structure, is greatly restricted at higher pH. This causes the ligand to escape, destroying the complex. This effect is probably also cooperative as the helix unravels gradually under the presence of –OH as more stabilizing hydrogen bonds are eliminated. One must also note that the single helix is less stable than the double helical structure of the B type crystals, which would account for the observed greater rate of displacement of the peak related to the complexed crystals relative to that of the B crystals.

The variation of the band position at lower pH shown in Fig. 4B is very similar to that observed in Fig. 4A, the type B crystalline peak. The explanation is similar; the helix acts as a shield against the hydrolyzation of the acetyl bond, while hydrolyzation takes place outside the crystal increasing the mobility of the free chains and the strain on the crystal (shift in band position to higher wavenumbers). By comparison with Fig. 4A, one notes that this position displacement is less pronounced for the complexed crystals than for the peak associated with the type B crystals, again suggesting that the double helix is more stable and a better shield than the single helical structure. The abrupt hydrolyzation of the acetyl bonds involved in the helix corresponds with a rapid shift to lower wavenumbers. This attack of the helix begins, as in Fig. 4A, at a pH of 3.

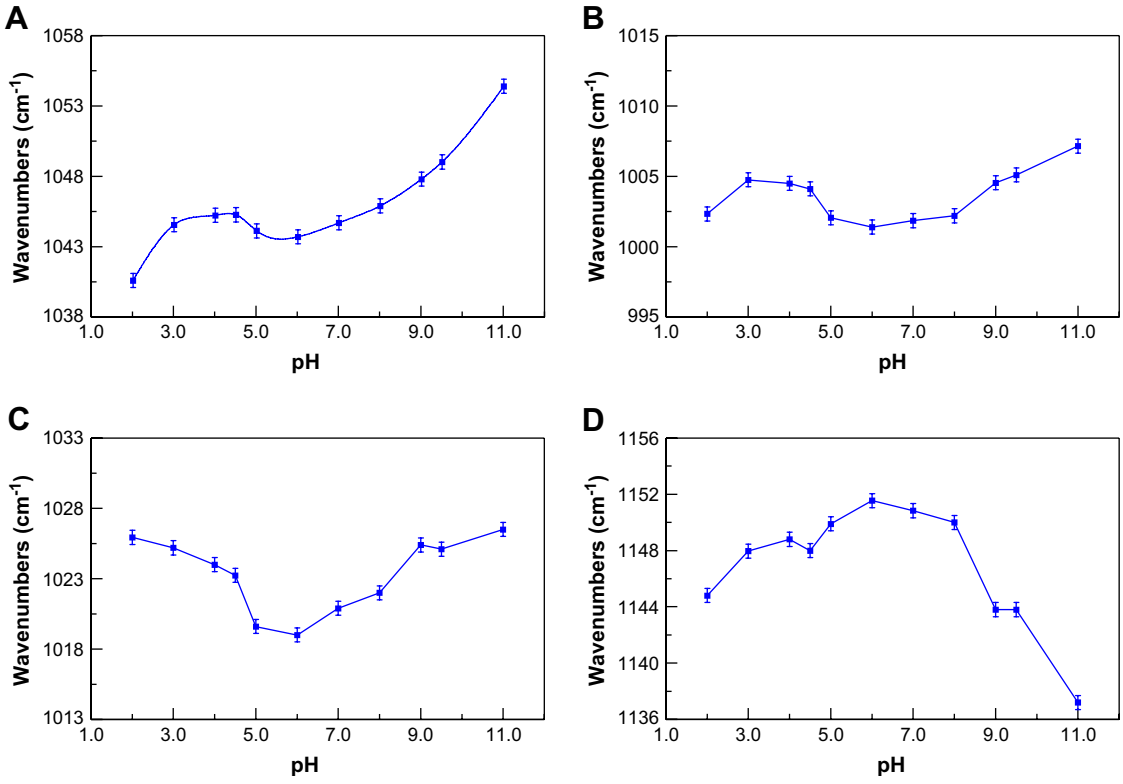

Fig. 4. Variation IR positions of four peaks, determined after spectral simulation, with increasing pH. See text for details. The error bars represent the standard deviation from at least five samples.

Although the peak position variation as a function of pH follows our hypothetical assignment, the similarities between Fig. 4A and 4B make it difficult to positively assign either band to the type B or to the complexed crystals environment, based solely on this data.

The position displacement of the band attributed to the C–O vibrations in an amorphous environment is shown in Fig. 4C. The variation observed is significantly different than that of the crystalline bands. As expected from Fig. 4A and 4B, at a pH higher than 6, a shift towards higher wavenumbers is observed, which can be explained by the decrease in the number of intra- and intermolecular hydrogen bonds. The fact that relatively few intramolecular hydrogen bonds are found in the amorphous phase compared to crystalline regions, explains that the increase is relatively smaller than those found in the peaks related to either crystalline phases. Very little tension is produced by the disruption of the surrounding hydrogen bonds. What little strain is observed probably comes from the neighborhood entanglements.

The most significant difference between the position shift of the crystalline bands and the amorphous-related peak is found at lower pH. Fig. 4C clearly shows an increase in wavenumbers for this later as the pH diminishes to values lower than 5. Since this band responds differently than the others to the same stimulus it must occur in a significantly different vibrational environment. The increase in the 1022 cm^{-1} band at lower pH can be explained by supposing that the amorphous phase is surrounded by crystalline and network regions, which stabilize the free parts of the hydrolyzed chains occurring in the amorphous phase. The small but steady strain caused by this pull causes the small shift to higher wavenumbers. The observed shift is relatively small although not negligible.

Lastly, Fig. 4D represents the variation with pH of a band tentatively associated with physical entanglements, forming networks. The abrupt shift to lower wavenumbers observed at pH higher than 8 is indicative of the importance of the hydrogen bonds to the stabilization of the entanglements, the release of these "safety hooks" enables the relaxation of the tension in the knots and possibly the eventual disentanglements of the chains. At a pH lower than 6, a steady decrease in the peak position is observed. Based on an analogy with polyolefins [15,21], where it was found that the regions of entanglements are more apt of be oxidized because of the higher chemical potential found there, the tension in the entanglements makes these sites more chemically active than the rest of the polymer. The hydrolyzation of acetyl bonds in this region will take place to release the knots and destroy the physical network. The free C–O are then vibrating at a frequency close to their unencumbered state. The variations observed for this band are in accordance with this hypothesis; therefore this band would seem mainly related to C–O vibrations in the physical network region in amylose.

The discussion above shows that an evaluation of the phase composition of amylose may also be obtained using IR. In the next step of our study, we will vary the phase composition and especially the network phase content and show the importance of the latter on the properties of amylose.

3.3. Polarization spectroscopy

The interest of polarized IR spectroscopy lies in the very different mobilities of the three types of phases analyzed. Under an external pressure, the amorphous phase will tend to follow the direction of strain while the network phase will follow more slowly with the crystalline phase, with its very low mobility, being the least affected. However, if, after a certain amount of time has elapsed, the external pressure is relieved, the crystalline phase is likely the stay in its position while the amorphous phase will immediately relax and the network phases will shift to a state intermediate between being fully oriented and randomly oriented.

Based on these assumptions, a fixed pressure in the form of a shear for 20 min was applied to samples containing a 30% V/V amount of an aqueous solution that had a specific pH. Upon release

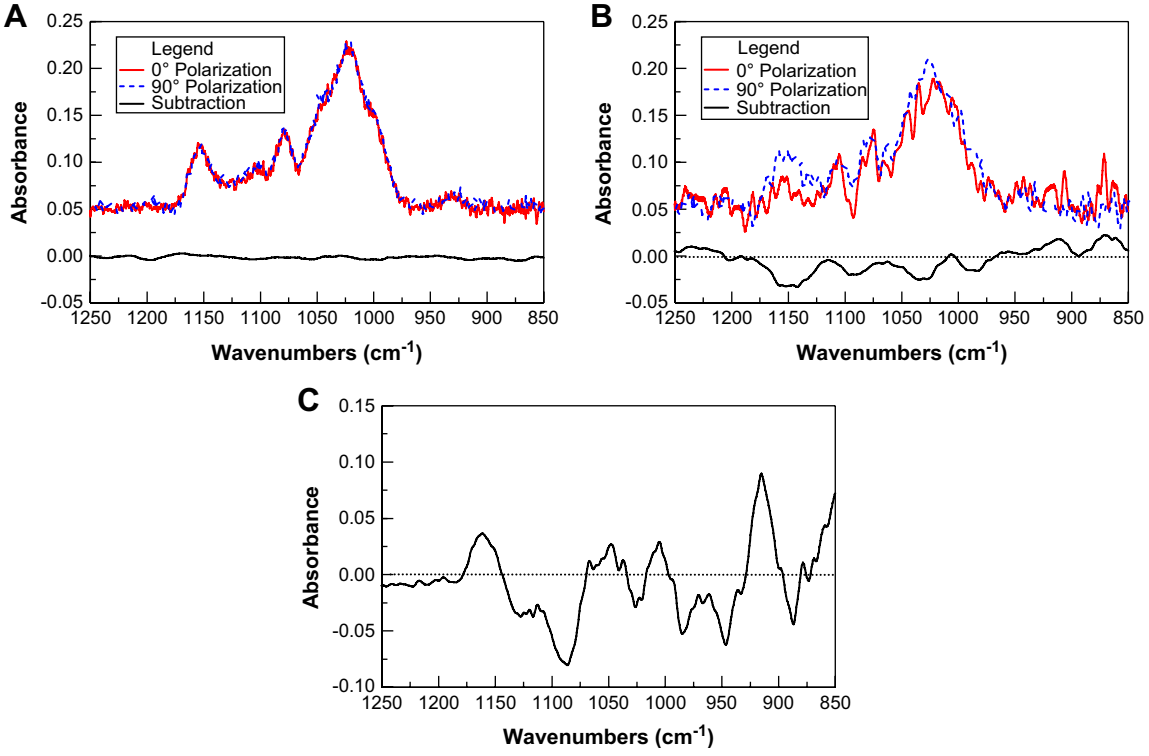

Fig. 5. Effect of IR light polarization on the spectra of amylose at various pH. (A) pH = 3; (B) pH = 6.5; (C) pH = 10.5. Note that for clarity only the subtraction between the spectra (polarized 0° − polarized 90°) is shown for C.

of the pressure, the sample was analyzed under polarized IR radiation both parallel and perpendicular to the shear direction. Fig. 5 shows the result of these measurements at pH 3 (A), pH 6 (B), and pH 10.5 (C). Both the parallel and perpendicularly polarized spectra are given with their subtraction presented in the lower part of the figure. Pressure applied to a sample in water of pH 3, Fig. 5A, does not significantly modify the spectra in any specific direction. This observation confirms the hypothesis that the low pH hydrolyses the acetyl bonds in the regions of crystalline and network content, increasing the mobility of all regions and permitting their rapid relaxation after the pressure is released.

A more neutral pH of 6.5, Fig. 5B, permits to distinguish the various phases as expressed by their different mobilities. The subtraction shows six divergences between the two spectra. Two unidentified bands around 920 and 865 cm^{-1} show an increase in the spectra oriented parallel (0° orientation) to the direction of shear. An increase in the spectra perpendicularly (90° orientation) was also observed around the 1150 and 1100 cm^{-1} position. The first was previously attributed to the C–O stretching vibrations related to the physical network while the second may be related to a similar vibration in a hydrogen bond network environment. One must note that the band positions resulting from the subtraction may vary from the original band assignments. If the treatment causes the bands to shift positions slightly or to become wider or narrower, the subtracted spectra may have a maximum or a minimum at a position where no band existed before. When unclear, we relied on spectra simulations to determine which peaks were most influenced by the specific treatments. If the chains follow the direction of the shear, an increase in absorbance will be expected in the perpendicularly polarized spectra. These results suggest that the networks both follow the direction of shear. Based on the hypothesis that all the bands in this region of the spectra (1300–800 cm^{-1}) possess similar absorptivity coefficients, the intensity of orientation, measured by the absolute value of the difference between the two spectra, is about twice as large for the physical network than for the hydrogen bond network. This might at first be surprising, but considering the fact that the hydrogen bonds outnumber by far the amount of entanglements and that these later are probably found in the amorphous, mobile region, while the hydrogen bond network is mainly in the crystalline, less mobile region. The presence of a shear stress is expected to orient the amorphous regions first, orienting the entanglements in its wake.

Fig. 5B also shows negative peaks at 1030 and 980 cm^{-1}, which are thought to belong to the type B and complexed crystals, respectively. This shift in position suggests not only an orientation in the direction of the shear but also a deformation of the C–O bond. However, their intensity of orientation differs in that the complexed crystal orients 1.5 times as much as the type B crystals. One also notes that the hydrogen bond network intensity of orientation is similar to that of the type B crystals, in accordance with the hypothesis that both are found in the same region of space. The difference between the two types of crystallinity can be understood by assuming that the rigidity of a single chain helix is more deformable than a double helix. One must note that the time of the experiment is also important as the chains under stress may eventually relax into an un-oriented structure.

In Fig. 5C only the difference between the spectra is shown in order to clarify the graph. At a pH of 10.5, the mobility of the different phases is more varied. The bands around 920 and 850 cm^{-1} are clearly even more oriented than before, again in a direction perpendicular to the applied pressure. The crystalline related bands also exhibit the same orientation as before, although much more strongly than at a lower pH. They are also broader which results in a more complex difference spectrum. This broadening may be explained by the larger distribution of vibrations in different strained environments. At this pH the complexed crystal band is found to be less oriented than that of the type B crystal band. This is probably caused by the fact that the amount of type B crystals present is much larger than that of the complexed type, as was confirmed by X-ray crystallography.

Fig. 5C also shows that the band associated with the hydrogen bond network is now strongly oriented in the same direction as the shear. At this pH most of the hydrogen bonds are eliminated. Two explanation of this orientation exist: the simplest is that this peak contains a secondary contribution related to the crystalline phase. A second hypothesis is that the hydrogen bonds remaining are those that are the best protected, i.e. imbedded in the double helix of the crystals. Therefore, when the crystals orient, these hydrogen bonds follow. The band corresponding to the entanglements in also oriented but at this pH it changes orientation as seen by the positive peak in Fig. 5C. The entanglements involved at this pH must be very close to the crystalline chains so that their disentanglement is difficult. This proximity might permit the knots only one orientation, that of being perpendicular to the crystal chain and the direction of shear. To further conclude on the variation of the two network bands the complete region of pH must be analyzed.

The absorbance differences of each band of interest in the 0° – 90° polarized light spectra are given in Fig. 6. As expected, the amorphous band is seen to be only slightly oriented whatever the pH. The type B crystals are non-oriented at low pH with an orientation maximum found at a pH of 10.5. Once the hydrogen bonds stabilizing the crystals are eliminated, they relax from the

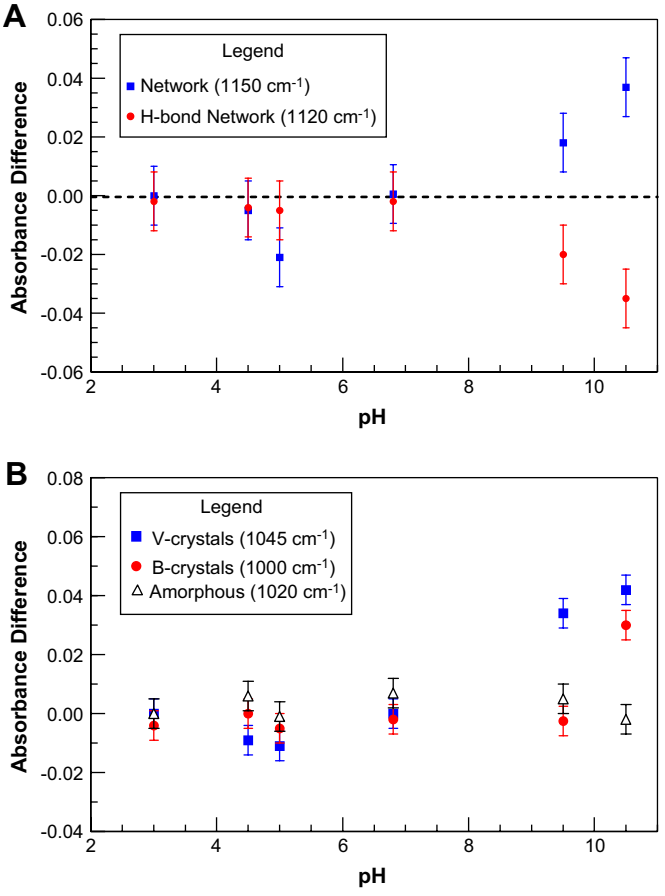

Fig. 6. Effect of pH on the difference in absorbance between bands with 90° polarization difference (polarized 0° – polarized 90°). In A, the variations in the bands associated with networks are presented, while in B, the variations in the bands associated with the crystalline and amorphous structures are presented. The error bars represent the standard deviation from at least five samples.

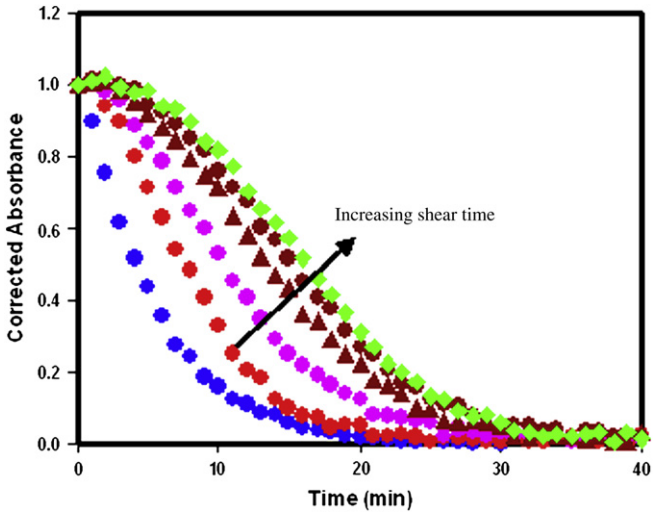

Fig. 7. Enzymatic biodegradation of the amylose–iodine complex of samples under different shear times.

tension caused by the shear and unorient themselves. A similar result is found for the single helix crystals but the orientation maximum is found at a lower pH, demonstrating the relative fragility of this structure. Furthermore, the fact that both types of crystals behave in an independent manner, points to the fact that both must be physically separated in space in the polymer so that no interactions can take place.

Fig. 6B also shows the orientation of the network phases with pH. The hydrogen bond network has a large plateau were the orientation is stable between a pH of 3 and 8. This network is released slowly when the pH reaches a value higher than 8. One notes that this network relaxes first, than both crystal phases relax which shows a possible interaction between the network of hydrogen bonds and the crystalline phase. A similar interaction is also possible between the physical network and the hydrogen bond network. As Fig. 6 shows, both phases vary in an identical manner at pH values lower than 6. However, at higher pH the physical network behaves distinctly as it orients itself perpendicularly to the axes of shear. The hydrogen network is therefore responsible for much of the morphology of amylose. Once it is partially eliminated, the physical network first is relaxed from the tension and is then reoriented while the single helix crystal is relaxed with the type B crystals shortly released thereafter.

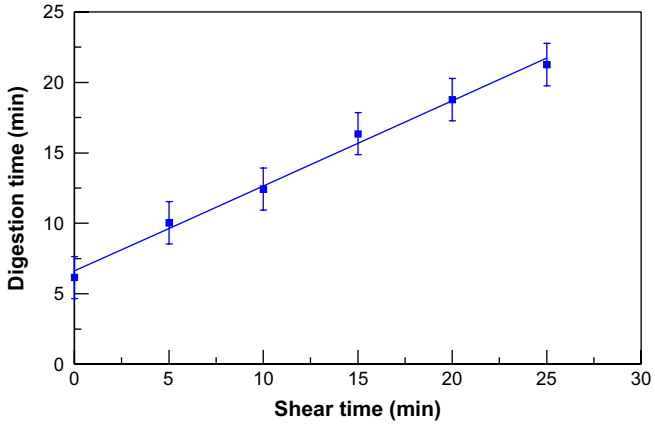

Fig. 8. Correlation of the characteristic digestion time determined from Fig. 7 as a function of time under shear stress.

3.4. Control of the physical properties through the network orientation

The importance of the network is evident when trying to control its contribution and relating it to a physical property. Using the well-known iodine complexation of amylose colorimetric method [38] the enzymatic digestion kinetics of untreated and treated samples were determined. One notes that this methodology involves adding a small amount of iodine to the amylose paste without completely dissolving the sample to retain orientation. Fig. 7 shows the resulting decrease in absorbance as a function of time for the digestion of shear stressed amylose samples for various times under shear. As the time of shear was increased, the digestion time increased. A correlation of the time of digestion, taken as the inverse of the first order reaction rate is plotted as a function of the amount of network phase in Fig. 8. A seemingly linear relationship is observed, which indicates the structural importance of the network phase on the physical properties of amylose. As the enzymatic degradation of amylose is closely related to the structure of the polycarbohydrate, Fig. 8 suggests that the network phase significantly affects the structure and behavior of the biopolymer.

4. Conclusion

Based on a three-phase model, consisting of crystalline (types B and V), amorphous and network (physical entanglements and hydrogen bond related) environments, we used isothermal DSC assisted by FTIR spectroscopy to observe the phase composition of amylose. Results suggest that the relative mobility of the chains in various environments (amorphous, crystalline and network) could be estimated by straining the sample and measuring the relaxation of each phase by IR.

Varying the pH of the water present in the samples enabled the gradual unraveling of the morphology of amylose and the detection of the presence of the networks. Such networks, preferentially located in the amorphous phase, were found to be more reactive to chemical and probably thermal modifications. However, when chain entanglements, or hydrogen bond networks, are found near or in the helix of the crystalline phase, the polymer is more resistant to chemical and physical modification. This allied to the fact that pH can be used to control the morphology and phase content of amylose can have a significant impact on the processing techniques of starch in numerous applications.

Acknowledgment

The partial supports provided by the Welch Research Foundation (grant V-0004) as well as by the Texas Coordinating Board, Advanced Research Program (003581-0001-2006) are gratefully acknowledged.

References

[1] Jane J. Journal of Macromolecular Science: Pure and Applied Chemistry 1995;A32:751–7.
[2] Mulhbacher J, Mateescu MA. International Journal of Pharmaceutics 2005;297:22–9.
[3] Lenaerts V, Moussa I, Dumoulin Y, Mebsout F, Chouinard F, Szabo P, et al. Journal of Controlled Release 1998;53:225–34.
[4] Kizil R, Irudayaraj J. Journal of Agricultural and Food Chemistry 2006;54:13–8.
[5] Maaurf AG, Man YBA, Asbi BA, Junainah AH, Kennedy JF. Carbohydrate Polymers 2001;45:335–45.
[6] Tananuwong K, Reid DS. Journal of Agricultural and Food Chemistry 2004;52:4308–17.
[7] Moorty SN, Andersson L, Eliasson AC, Santacruz S, Ruales J. Starch/Starke 2006;58:209–14.
[8] Lewen KS, Paeschke T, Reid J, Molitor P, Schmidt SJ. Journal of Agricultural and Food Chemistry 2003;51:2348–58.
[9] Baik MY, Kim KJ, Cheon KC, Ha YC, Kim WS. Journal of Agricultural and Food Chemistry 1997;45:4242–8.

[10] Silverio J, Svensson E, Eliasson AC, Olofsson G. Journal of Thermal Analysis 1996;47:1179–200.
[11] Roesser DS, McCarthy SP, Gross RA. Macromolecules 1996;29:1–9.
[12] Kizil R, Irudayaraj J, Seetharaman K. Journal of Agricultural and Food Chemistry 2002;50:3912–8.
[13] Tester RF, Karkalas J, Qi X. World's Poultry Science Journal 2004;60:186–95.
[14] Brady JE, editor. Matter and its changes. 3rd ed. New York: Wiley; 2000.
[15] Bernazzani P, Chapados C, Delmas G. Journal of Polymer Science, Part B: Polymer Physics 2000;38:1662–77.
[16] Biliaderis C, Can G. Journal of Physiology and Pharmacology 1991;69:60–78.
[17] van Soest JJG, de Wit D, Tournois H, Vliegenthart FGJ. Carbohydrate Research 1995;279:201–14.
[18] Nuessli J, Sigg B, Conde-Petit B, Escher F. Food Hydrocolloids 1997;11:27–34.
[19] Conde-Petit B, Nuessli J, Handschin S, Escher F. Starch/Starke 1998;50:184–92.
[20] Hulleman SHD, Helbert W, Chanzy H. International Journal of Biological Macromolecules 1996;18:115–22.
[21] van Soest JJG, Hulleman SHD, de Wit D, Vliegenthart JFG. Carbohydrate Polymers 1996;29:225–31.
[22] Akuzawa S, Sawayama S, Kawabata A. Bioscience, Biotechnology, and Biochemistry 1997;61(3):487–90.
[23] Cheetham NWH, Tao L. Starch/Starke 1997;49:407–15.
[24] Cheetham NWH, Tao L. Carbohydrate Polymers 1998;35:287–95.
[25] van Soest JJG, de Wit D, Tournois H, Vliegenthart FGJ. Polymer 1994;35:4721–7.
[26] van Soest JJG, de Wit D, Tournois H, Vliegenthart FGJ. Starch/Starke 1995;46:453–7.
[27] Bernazzani P, Delmas G. Journal of Thermal Analysis 1997;49:449–54.
[28] Bernazzani P, Bich VT, Nguyen HP, Haine A, Chapados C, Le HD, et al. Canadian Journal of Chemistry 1998;76:1–14.
[29] Zhang X, Nguyen HP, Bernazzani P, Lapes I, Delmas G. Canadian Journal of Chemistry 1997;75:1354–62.
[30] Imberty A, Perez S. Biopolymers 1988;27:1205–21.
[31] Tako M, HiZukuri S. Journal of Carbohydrate Chemistry 1995;14:613–22.
[32] Kondo T, Sawatari C. Polymer 1994;35:4423–8.
[33] Kondo T, Sawatari C. Polymer 1996;37:393–9.
[34] Bernazzani P, Chapados C, Delmas G. Biopolymers 2001;58(3):305–18.
[35] Snyder RG, Liang GL, Strauss HL, Mendelsohn R. Biophysical Journal 1996;71:3186–98.
[36] Godet MC, Bizot H, Buleon A. Carbohydrate Polymers 1995;27:47–52.
[37] Godet MC, Bouchet B, Colonna P, Gallant DJ, Buleon A. Journal of Food Science 1996;61:1196–201.
[38] Zhang G, Venkatachalam M, Hamaker BR. Biomacromolecules 2006;7:3259–66.